Jeong *et al.*
Journal of Analytical Science and Technology (2023) 14:27
https://doi.org/10.1186/s40543-023-00384-3

Journal of Analytical Science and Technology

RESEARCH ARTICLE

Open Access

Mass spectrometry-based metabolomics study for delay tomato fruit ripening by sound waves

Mi-Jeong Jeong[1*†], Byoung Joon Ko[2†] and Joo Yeol Kim[1]

Abstract

Tomato (*Solanum lycopersicum* L.) is one of the most consumed vegetables worldwide. The ripening of tomato is performed for its freshness and represented by color and gene expression. In our previous study, we performed molecular analyses on tomato ripening with and without sound-wave treatment. In the present study, we performed metabolomics analysis of ripening tomatoes with and without sound-wave treatment to expand our knowledge of tomato ripening. To achieve this goal, tomatoes at 7, 10, and 14 d of ripening were selected and analyzed via liquid chromatography–mass spectrometry (LC–MS) and gas chromatography–MS (GC–MS). A total of 33 major metabolites, including 14 LC–MS- and 19 GC–MS-derived metabolites, were assigned based on variable importance projection and *p* values and subjected to statistical analysis. Apparent morphology and partial least squares–discriminant analysis were consistent with the general ripening process based on color. Moreover, metabolomics analysis showed similar experimental results to those of previous studies. The quantification of metabolites with LC–MS showed decreasing levels of adenosine, tryptophan, and phytosphingosine upon sound-wave treatment. In GC–MS analysis, 4-Aminobutanoic acid and aspartic acid were decreased upon sound-wave treatment. On the other way, the quantity of malic acid, citric acid, and sucrose was increased with the treatment. The findings of this study can assist in the application of sound-wave treatment for delaying ripening in tomatoes and improving their market value.

Keywords Sound wave, Tomato ripening, Metabolites, Liquid chromatography–mass spectrometry, Gas chromatography–mass spectrometry

Introduction

Tomato (*Solanum lycopersicum* L.) is one of the most consumed vegetables worldwide because it is considered healthy and nutritious (Zhang et al. 2019). The tomatoes' antioxidant, anti-inflammatory, and anti-cancer properties have been extensively studied (Fiedor and Burda. 2014). The ripening process after harvest affects the quality of tomatoes, which undergoes many metabolic changes and the regulation of gene expression. In addition, the ripening process makes tomatoes edible and enhances their flavor (Wang et al. 2020). Since the ripening process gradually deteriorates fruits, a controllable and delayed ripening process is desirable. Thus, many studies have focused on maintaining and improving the quality of tomatoes by elucidating their ripening process.

Ethylene is considered a major factor related to ripening in tomatoes and has been widely investigated. It is a plant hormone that is involved in senescence and affects growth, development, and ripening (Matto and Suttle. 1991; Abeles et al. 1992). S-adenosylmethionine is a

†Mi-Jeong Jeong and Byoung Joon Ko contributed equally to this work

*Correspondence:
Mi-Jeong Jeong
center1097@korea.kr
[1] Department of Agricultural Biotechnology, Rural Development Administration, National Institute of Agricultural Science, 370 Nongsaengmyoeng-ro, Deokjin-gu, Jeonju, Jeollabuk-do 54874, South Korea
[2] School of Biopharmaceutical and Medical Sciences, Sungshin Women's University, 01133 Seoul, South Korea

precursor for ethylene biosynthesis and is converted into 1-aminocyclopropane-1-carboxylic acid (ACC) by ACC synthase (ACS) and ACC oxidase (ACO), which catalyze the synthesis of ethylene associated with the ripening process in tomatoes (Johnson and Ecker. 1998). In the process of ripening, the expression of several ethylene biosynthesis-related genes, including *LeACS2*, *LeACS4*, and *LeACO1*, dramatically increases, indicating that these genes are key regulators of ripening (Hoogstrate et al. 2014). As other key factors for tomato ripening, ethylene-inducible genes, *E4* and *E8*, show decreased and increased expression in response to ethylene, respectively (Kesanakurti et al. 2012). In addition, ripening inhibitors (RINs), including colorless non-ripening (CNR) and non-ripening transcription factor (NOR), play an important role upstream of the ethylene production pathway in fruit ripening (Vrebalov et al.2002; Giovannoni. 2004; Manning et al. 2006). In particular, RINs regulate gene expression by binding to the promoters of *ACS* and *ACO* in tomatoes (Kesanakurti et al. 2012). Moreover, the tomato agamous-like 1 (*TAGL1*) gene plays an important role in fruit expansion and ripening as an important regulatory factor (Pan et al. 2010). Our previous work proved that negatively regulating ethylene biosynthesis via sound-wave treatment delays tomato ripening. Real-time quantitative polymerase chain reaction analysis showed that tomato ripening is affected by the expression levels of several ethylene biosynthesis genes, such as *ACS2*, *ACS4*, *ACO1*, *E4*, and *E8*, and ripening-related transcription factors, such as RIN, TAGL1, hemoglobin 1 (HB-1), NOR, and CNR. In addition, these genes are influenced by sound-wave treatment throughout 15 d of ripening (Kim et al. 2015).

Sound is an external signal in the form of molecular vibrations transmitted via various media, and the mechanism of the plant response to sound remains unclear (Gagliano et al. 2012; Shipman et al. 2016). In a recent study, we reported that specific sound waves delayed fruit ripening, promoted plant growth, and increased the production of functional metabolites, such as vitamin C and flavonoids (Kim et al. 2017, 2020). These results suggest that appropriate sound-wave treatment in plants can regulate gene expression and metabolite synthesis. Sound waves promote the growth of *Arabidopsis* roots, rice, and cucumber seedlings (Takahashi et al. 1991; Johnson et al. 1998; Kim et al. 2021); regulate the level of plant growth hormones in *Chrysanthemum* (Bochu et al. 2004; Kim et al. 2021); and induce the development of resistance to abiotic and biotic stresses (Wang et al. 2003; Choi et al. 2017).

Metabolomics studies using liquid chromatography-mass spectrometry (LC–MS) and gas chromatography-mass spectrometry (GC–MS) have been widely performed to identify and quantify metabolites from various sources (Yang and Hoffman. 1984; Wishart. 2019). Recently, untargeted metabolome analysis could produce 7,188 accurate mass values and identified 1,577 metabolites in tomato samples (Ara et al. 2021). Further, Mun et al. (2021) performed a non-targeted metabolomics study using five tomatoes from different regions to evaluate regional differences. A metabolic pathway map of tomatoes was built to infer metabolic differences among these tomato varieties. Zhang et al. (2019) also analyzed tomato metabolomes and transcriptomes to identify transcription factors affecting tomato fruit quality. They independently analyzed tomato samples and reported the accumulation of alpha-tomatine in fruits based on metabolic studies. In contrast, the metabolomics aspects of the effect of sound-wave treatment on tomato ripening remain unknown. Thus, an accurate experimental design and precise metabolomic analysis are needed to deduce the key metabolites associated with the tomato ripening process and the effect of sound-wave treatment.

In the present work, we compare the tomato metabolites with and without 1-kHz sound-wave treatment at 7-, 10-, and 14-d ripening. A total of 29 metabolites were identified and analyzed with statistical analysis such as PLS-DA. Variable importance in the projection (VIP) values provided by PLS-DA was used for finding metabolites related to the ripening process. Based on findings from this study, several metabolites provide supportive evidence that sounds wave treatment delay of tomato ripening.

Materials and methods

Materials

LC–MS-grade methanol, acetonitrile, and water were obtained from Thermo Fisher Scientific (Hampton, NH, USA) and used without further purification. Other reagents, including hydroxymethoxy amine and N, O-bis (trimethylsilyl)trifluoroacetamide (BSTFA), were purchased from Sigma–Aldrich (St. Louis, MO, USA).

Plant materials and treatment conditions

Tomato (*Solanum lycopersicum* L.) fruits were collected at the mature green stage of development (average weight, 172.9 ± 1.7 g) from a commercial greenhouse facility in Jeongeup and Yong-In, South Korea. The sampled tomato fruits were exposed to a sound wave with a frequency of 1 kHz for 6 h. A single-frequency wave was generated using Pro Tools M-Powered software (Avid Technology, Burlington, MA, USA). The speaker volume was 100 dB, and the experiments were performed in a custom-made soundproof chamber (Korea Scientific Technique Industry Co., South Korea) to prevent exposure to external noise. The sound level within the chamber was fixed at

approximately 40 dB, whereas the sound level in a commercial growth chamber typically reaches approximately 80 dB. The tomato fruits were placed in the soundproof chambers to prevent vibration transfer among the tomatoes during sound-wave treatments. The treatment and control groups were maintained at 23 ± 1 °C, following storage at 23 ± 1 °C. Changes in quality were monitored at 7, 10, and 14 d.

Metabolite preparation, LC–MS analysis, and GC–MS analysis

For LC–MS analysis, metabolites from powdered samples (20 mg) were extracted using 800 µL of 80% methanol using a homogenizer (Bioprep-24; Allsheng, Hangzhou, China), followed by sonication for 5 min at room temperature and centrifugation at 14,000 rpm for 10 min at 4 °C. The supernatant was injected for LC–MS analysis. Three biological replicates were analyzed, and the average result was calculated in both LC–MS and GC–MS analyses. The extracted and prepared metabolite samples were separated on a Waters ACQUITY I class UPLC system (Waters, Milford, MA, USA) using an ACQUITY BEH C18 column (2.1 mm × 100 mm, 1.7 µm particle size). The mobile phase consisted of 0.1% formic acid in water (eluent A) and 0.1% formic acid in acetonitrile (eluent B) in the gradient mode at a flow rate of 0.35 mL/min. The gradient applied was: 0–1 min, 10% eluent B; 1–8 min, linear increase to 100% eluent B; 8–9.5 min, 100% eluent B; 9.5–10 min, linear decrease to 10% eluent B at 0.35 mL/min. The eluate was analyzed in positive mode using a Waters G2-XS Q-TOF mass spectrometer equipped with an electrospray ionization source operating in positive mode over m/z 50–1,500 range with a scan time of 0.2 s. The capillary voltage was set at 3 kV with sample cone voltage of 30 V. The flows of desolvation gas and cone gas were 800 L/h and 30 L/h, respectively. The ion source temperature was at 100 °C, and the desolvation temperature was at 400 °C.

For GC–MS analysis, 80% methanol was added to tomato fruits to a final concentration of 0.02 g/mL. The samples were then centrifuged at 14,000 rpm for 10 min. Subsequently, 10 µL of the supernatant was completely dried using CentriVap (Labconco, Kansas City, MO, USA). Derivatization was performed by adding 70 µL of hydroxymethoxy amine to the samples and reacting at 37 °C for 90 min. BSTFA (70 µL) was added, and the mixture was incubated at 70 °C for 30 min. The derivatized samples were centrifuged at 14,000 rpm for 10 min, and the supernatant was injected for GC–MS analysis. To separate the derivatized metabolites, a Shimadzu GC-2010 Plus system (Shimadzu, Tokyo, Japan) equipped with a DB-5 MS column (30 m × 0.25 mm, 0.25 µm film thickness; J&W Scientific, Santa Clara, CA, USA) was used for the separation. The flow rate of the helium carrier gas was 1 mL/min, and the split ratio was 40:1. The injector temperatures were 200 °C. The oven was programmed to hold for 2 min at 70 °C, increase to 210 °C at 7 °C/min, increase to 320 °C at 10 °C/min, and then hold at 320 °C for 7 min. For GC–MS analysis, a GCMS-TQ 8030 mass spectrometry interfaced with Q3 scan mode was used for MS-based spectral identification and quantification. The ion source and interface temperatures were 230 °C and 280 °C, respectively. The detector voltage was 0.1 kV, and event time was 0.03 s at 15 eV. A mixture of all samples was injected after every six samples for quality control.

Metabolite identification, quantification, and statistical analysis

The LC–MS results were collected and aligned using MassLynx software (Waters). The collected data using peak-to-peak baseline noise of 1, noise elimination of 6, peak-width at 5% height of 1 s, and an intensity threshold of 50,000 were aligned with a 0.05 Da mass window and 0.2 min retention time window. Metabolite identification with aligned data was performed against Chemspider (www.chemspider.com), Metlin (metlin.scripps.edu), and human metabolome database (www. hmdb.ca). NIST 11 and Wiley 9 mass spectral libraries were used for identification of the metabolites in GC–MS data. In addition, retention indices (RIs) were also used for the identification. The collected LC–MS and GC–MS data were processed using the UNIFI (Waters) and GC–MS solution systems (Shimadzu), respectively. Fourteen and nineteen specific metabolites assigned from LC–MS and GC–MS data were quantified using peak areas; then, partial least squares discriminant analysis (PLS-DA) was performed to discern differences among the groups using SIMCA-P + version 16.0.2 (Umetrics, Umeå, Sweden). PLS-DA provides variables important in projection (VIPs), which explain the intergroup variation. Finally, the boxplots were drawn using the R-project.

Results and discussion

Morphological and physicochemical differences

In a previous study, we showed that tomato ripening along with the expression of ethylene biosynthesis-related genes (*ACS2*, *ACS4*, *ACO1*, *E4*, and *E8*) and ripening-related genes (*RIN*, *TAGL1*, *HB-1*, *NOR*, and *CNR*) is affected by sound-wave treatment (Kim et al. 2015). In this study, we extended our study from genomic analysis to metabolomics analysis using mass spectrometry. Before sample selection and metabolite extraction, we examined morphological differences between tomatoes with and without sound-wave treatment (Fig. 1). The proportion of green fruits was calculated during the ripening

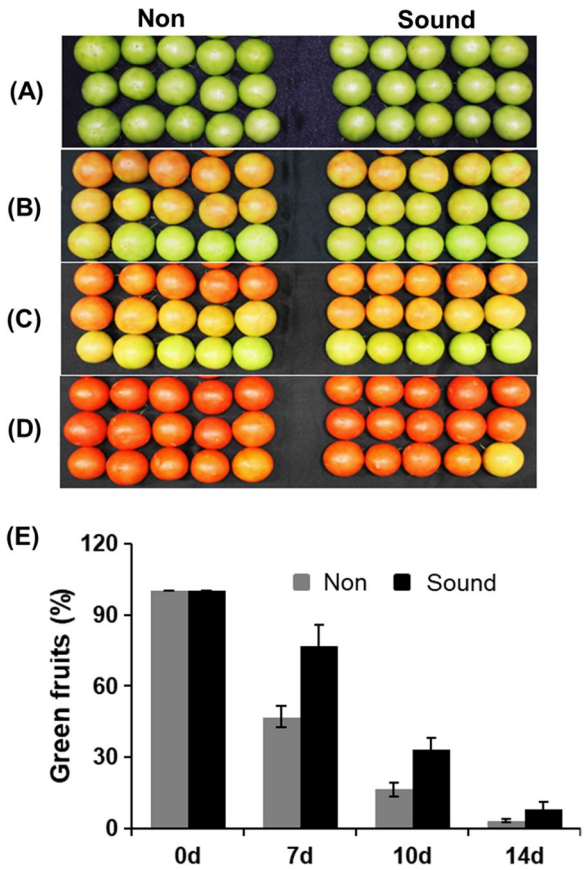

Fig. 1 Delayed ripening of tomatoes mediated by sound-wave treatment at 1 kHz. The morphological changes in ripening are shown with respect to the color of the tomatoes at **A** 0, **B** 7, **C** 10, and **D** 14 d after harvest. **E** Proportion of green tomato fruits during the 14 d following sound-wave treatment (1 kHz). Non, control; Sound, sound-wave treatment

process for up to 14 d. During ripening, the extent of red color was lower in tomatoes treated with 1-kHz sound waves than that in control tomatoes, while there was no considerable difference in color between the control and treated tomatoes during the 0-d ripening period. The morphological traits indicated delayed ripening upon 1-kHz sound-wave treatment (Fig. 1). For the metabolomics study, we collected samples at three time points based on the color difference between tomatoes with and without sound-wave treatment. The 0-d tomato samples were excluded from this metabolomics study because the treated tomatoes were not considerably different from untreated tomatoes. Three tomatoes were chosen from each group as biological replicates for the subsequent metabolomics analysis. The morphological differences could be explained based on our previous study, wherein the sound-wave treatment was shown to affect ripening from 0 to 14 d (Kim et al. 2015). Although the early ripening analysis showed delayed ripening with sound-wave treatment, we chose 7-, 10-, and 14-d-ripened tomatoes for this study because the greatest color differences were observable on these days. Based on the color of the tomatoes, three biological replicates were selected and subjected to metabolite extraction for MS-based analysis.

Metabolite profiling of tomatoes using LC–MS and GC–MS

Metabolite profiling was performed using a UPLC–Q-TOF mass spectrometer and GC–MS to identify and analyze metabolites from the six different groups. The metabolite profiles of tomato samples from LC–MS and GC–MS analyses are shown in Fig. 2. In total, 147 and 25 peaks were detected in the LC–MS and GC–MS runs, respectively. However, only 14 metabolites were assigned as major metabolites for LC–MS (Table 1). The major metabolites shown in Table 1 were identified using elution time, molecular weight, and MS/MS fragmentation patterns from Chemspider and Metlin databases. Then, the metabolites were selected based on p value (<0.05) again except protein, LPC (18:2), and Cholesteryl acetate which were not shown as boxplot in Fig. 4. The VIP values of major metabolites in Table 1 were varied from 0.73 to 1.46. The total ion chromatogram generated via GC–MS is shown in Fig. 2, and assigned metabolites are listed in Table 2. Nineteen major metabolites were assigned the RI and NIST databases and were chosen based on the p values (<0.05). The VIP values of major metabolites in Table 2 were varied from 0.78 to 1.46. Unlike LC–MS, GC–MS data analysis used RI values along with molecular weight and MS/MS patterns for identification. The 14 major metabolites from LC–MS analysis comprised amino acids, flavonoids, LPC, and others. In contrast, the 19 major metabolites from GC–MS comprised organic acids, amino acids, and others. Although a recent study reported 1,577 metabolites derived from tomatoes (Ara et al. 2021), our current study evaluated only 14 and 19 major metabolites because fully confirmed metabolites should be considered for accurate statistical analysis.

Statistical analysis of LC–MS data

To evaluate the effect of sound-wave treatment on the tomato ripening process, we performed PLS-DA analysis with triplicate peak area data from LC–MS in which the CV% varied from 0.24 to 59.79%. The analytical reproducibility of LC–MS and GC–MS is shown in Additional file 1: Fig. S1 and Additional file 2: Fig. S2, respectively. The PLS-DA score plot based on LC–MS is shown in Fig. 3A, and total variability was 38.8% (t1-22.4%,

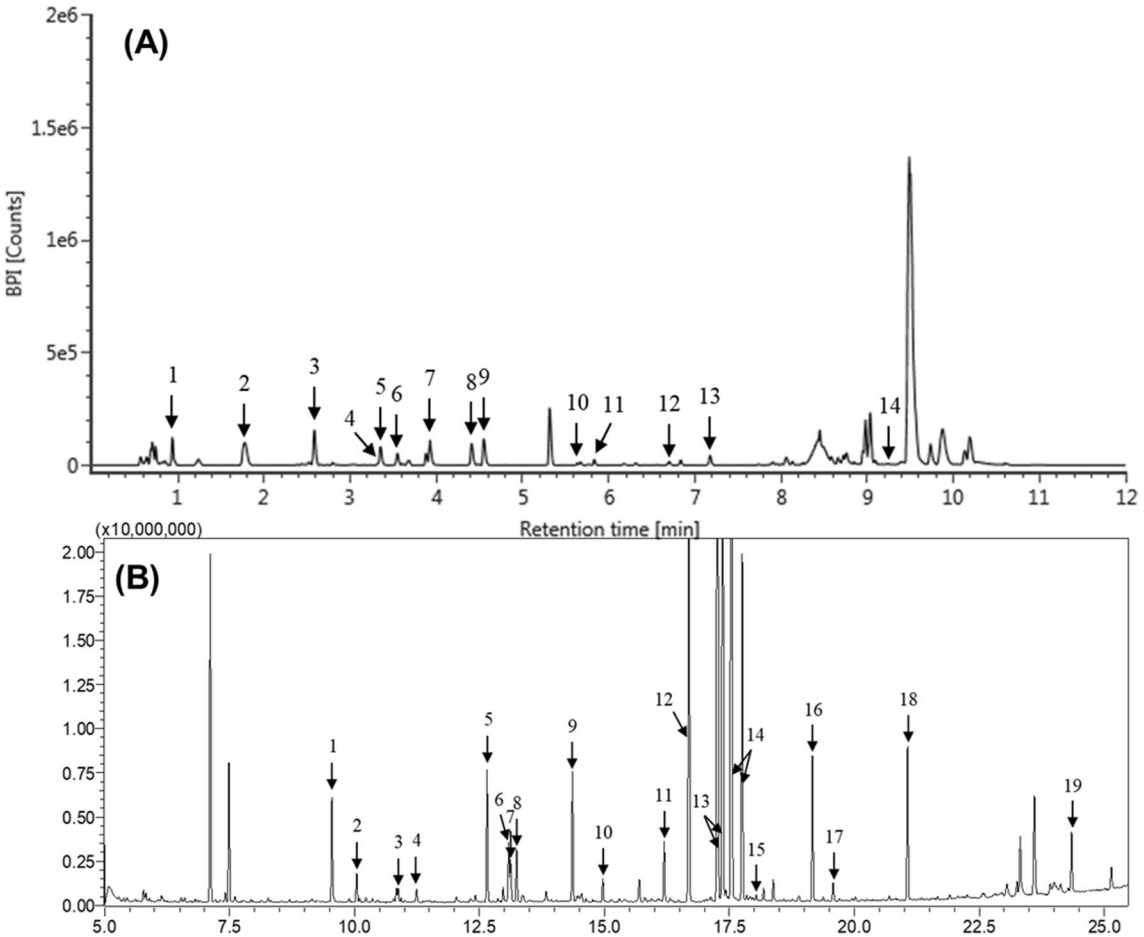

Fig. 2 Representative **A** LC–MS chromatogram for tomatoes using samples ripened for 7 d and **B** GC–MS chromatogram from one quality control sample. The numbers in the chromatograms represent the identified peaks matched with Tables 1 and 2. LC–MS, liquid chromatography–mass spectrometry; GC–MS, gas chromatography–mass spectrometry

t2-16.4%). Based on the PLS-DA model, total 11 metabolites were chosen among the 14 identified metabolites using variable importance in projection (VIP) values (>0.5) and p values (<0.05). Boxplots of the chosen 11 metabolites are drawn in Fig. 4. The quantities of several metabolites, including adenosine, tryptophan, and phytosphingosine, decreased with sound-wave treatment, while no metabolites showed increasing levels with the sound-wave treatment. Guevara et al. reported that tryptophan accumulation occurs during the ripening of red fruits. (Guevara et al. 2021) In the same study, the researchers also observed that phytosphingosine was more abundant in red fruits than in green fruits. Their study indicated that the levels of the two metabolites increase as tomato ripening progresses; thus, these results are consistent with our LC–MS boxplot results wherein sound-wave treatment disrupted the ripening process and reduced the production of tryptophan and phytosphingosine. The metabolic levels decreased in the treated samples compared with those in the controls, supporting our hypothesis that the sound-wave treatment delays tomato ripening. In addition, our results indicated that adenosine might be one of the indicators for the ripening process.

Statistical analysis of GC–MS data

The GC–MS metabolites quantification data were analyzed in the same manner used in LC–MS data analysis. The peak areas from triplicated GC–MS data were used for PLS-DA, and the CV% of the triplicate varied from 0.02% to 13.54%. Based on the PLS-DA results (Fig. 3B) including VIP values (>0.7) and p values (<0.05), total 18 metabolites were used for drawing boxplots shown in Fig. 5. The GC–MS quantitative analysis with statistical analysis showed that glutamic acid and aspartic acid levels were lower in the treated samples than in the

Table 1 Identification of major metabolites from LC–MS runs

No.	RT (min)	Category	Compound	Exact mass $[M+H]^+$	MS fragments	VIP	*p* value
1	1.06	Amino acids	Phenylalanine	166.0847		1.11	2.16E−03
2	1.55		Tryptophan	205.0964		1.16	2.71E−04
3	2.88	Flavonoids	Rutin	611.1594	287, 303	1.23	0.035
4	4.19		Nariiigenin	273.0747	119, 147, 153	1.12	4.79E−10
5	0.85	Others	Adenosine	268.1017	136	1.46	1.70E−08
6	2.95		Esculeoside A	1270.6125	814, 754, 652, 592	0.99	2.49E−03
7	3.17		Beta 1 hydroxytomatine	918.5097	652, 594, 432	0.91	2.80E−05
8	3.54		Protogracillin	1065.5529	741, 579, 417	0.97	1.29E−03
9	4.14		Protein	1093.2407		0.57	0.319
10	5.45		Myristic diethauolamide	316.2824		1.2	3.68E−04
11	5.67		phytosphingosine	318.2989	300, 282	1.09	1.12E−04
12	9.21		Cholesteryl acetate	429.3712	164, 165, 205	0.73	0.553
13	6.63	Lysophosphadti-dyl-choline	LPC(18:2)	520.3398	184	1.01	0.058
14	6.99		LPC(16:0)	496.3389	184	1.28	4.13E−05

The metabolites were identified based on elution time, *m/z*, and MS/MS pattern. LC–MS, liquid chromatography-mass spectrometry; RT, retention time; VIP, variable importance projection; LPC, lysophosphatidylcholine

Table 2 Identification of major metabolites from GC–MS runs

No.	RT(min)	Category	Compound	RT	VIP	*p* value
1	9.55	Organic acid	Phosphoric acid	1265	0.83	2.43E−13
2	10.04		4-Aniinobutanoic acid, 2TMS	1297	0.92	2.64E−05
3	12.65		Malic acid	1476	0.91	3.82E−16
4	13.25		4-Aniinobutanoic acid, 3TMS	1521	1.46	1.09E−05
5	16.69		Citric acid	1809	1.4	2.92E−11
6	19.17		Palmitic acid	2043	1.14	7.96E−11
7	21.07		Stearic acid	2241	1.06	3.66E−09
8	10.88	Amino acid	Serine	1354	0.86	1.62E−10
9	11.24		Threonine	1379	0.93	2.11E−10
10	13.09		Aspartic acid	1508	0.82	8.57E−13
11	14.37		Glutamic acid	1613	0.9	1.60E−17
12	14.97		Asparagine, 3TMS	1663	0.82	8.49E−12
13	16.2		L-Glutamine, 3TMS	1767	0.81	2.14E−17
14	18.04		Tyrosine	1933	1.22	7.53E−05
15	13.13	Others	Oxoproline	1511	0.81	4.43E−11
16	19.58		Myo-inositol	2084	1.37	5.93E−10
17	17.26/17.37		Fructose	1862	0.85	7.03E−11
18	17.54/17.76		Glucose	1887	0.78	4.73E−13
19	24.35		Sucrose	2625	1.49	3.67E−17

The metabolites were identified based on RI, *m/z*, and fragment ions. GC–MS, gas chromatography-mass spectrometry; RT, retention time; RI, retention index; VIP, variable importance projection

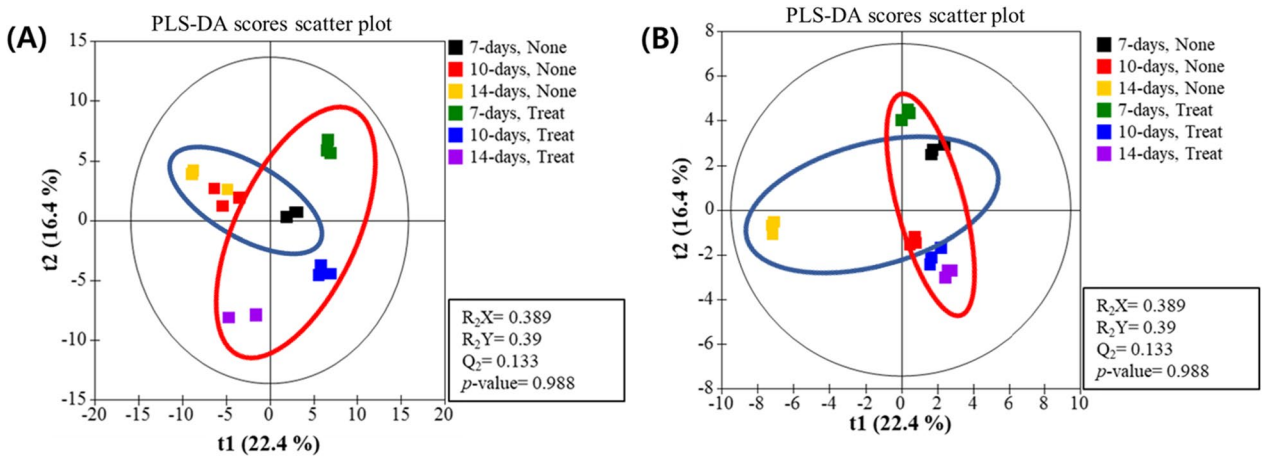

Fig. 3 PLS-DA score plots for **A** liquid chromatography-mass spectrometry results and **B** gas chromatography–mass spectrometry results. PLS-DA, partial least squares-discriminant analysis

controls. Our previous study showed that *TAGL1* plays a key role in the ripening process and increases the levels of several amino acids such as tyrosine, glutamic acid, and valine. Similar to our previous findings, levels of glutamic acid and tyrosine decreased in the treated samples, which contained relatively lower amounts of amino acids as the sound-wave treatment retarded ripening. In addition, fructose and glucose levels were higher in the control samples than in the treated samples. These results are consistent with the fact that ripen tomatoes are sweeter than green tomatoes. The levels of other organic acids such as phosphoric acid and 4-aminobutanoic acid decreased in the sound-wave treated tomatoes, whereas malic acid and citric acid levels increased in the treated tomatoes. The malic acid content in ripe fruits is fairly low, which agrees with the higher levels in the sound-wave-treated tomatoes (Agius et al. 2018).

Conclusions

Based on our previous study on the effect of sound-wave treatment on tomato ripening, we expanded the concept of delayed ripening via sound waves through metabolomics analysis. Tomatoes that ripened from 7 to 14 d were collected and prepared for LC–MS and GC–MS analyses. Although many metabolite peaks were annotated using the databases, a total of 32 major metabolites were identified based on VIP and *p* values, representing significant differences. LC–MS analysis showed that the levels of tryptophan and phytosphingosine decreased with sound-wave treatment. The levels of several amino acids and sugars determined via GC–MS are also in agreement with our previous findings and those of other studies. Sound-wave treatment was effective at delaying the ripening of tomatoes and regulating the production of several primary metabolites, corresponding with the results of other studies.

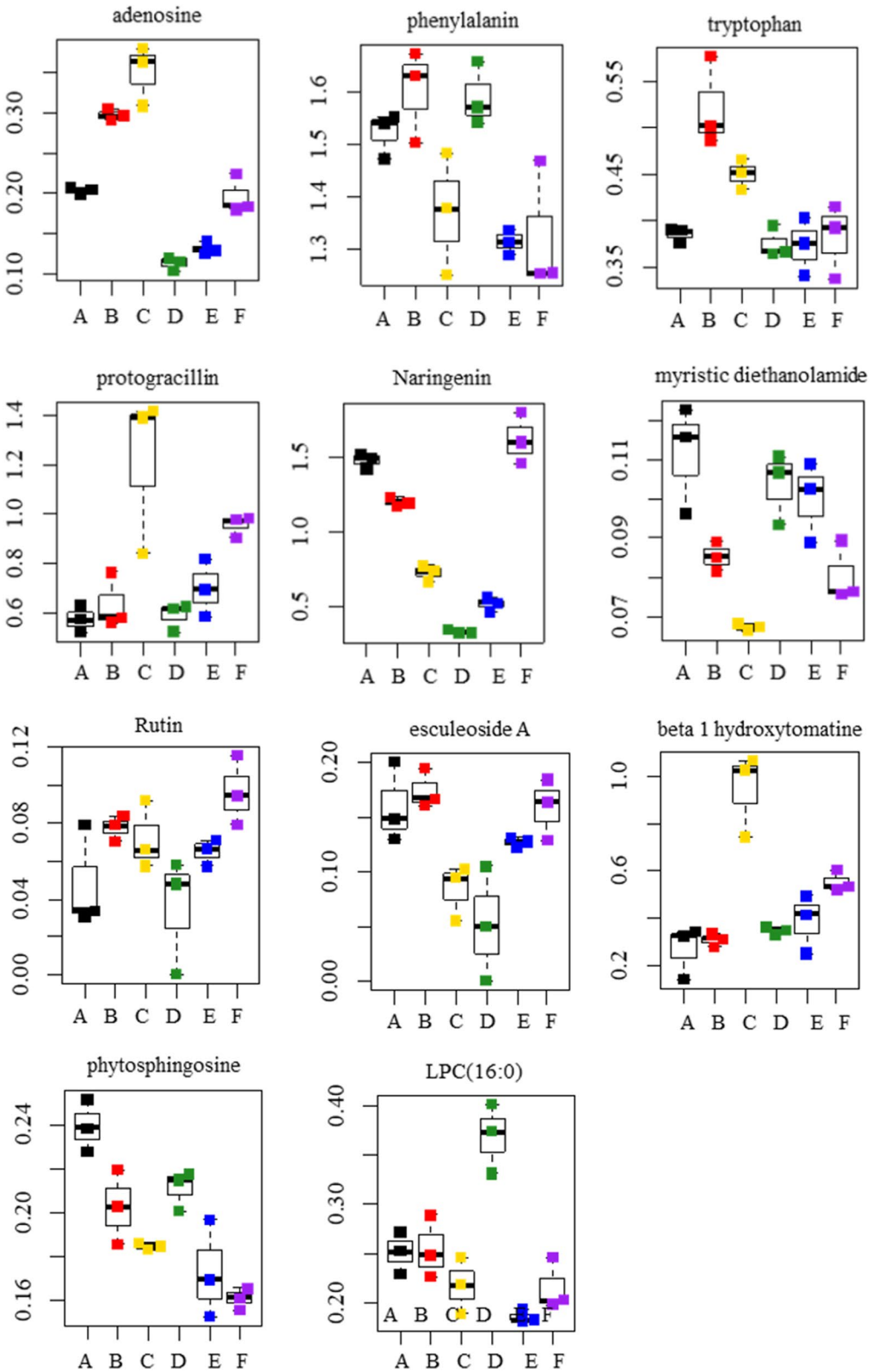

Fig. 4 Boxplot of each metabolite identified in LC–MS analyses. The 11 metabolites were quantified based on LC–MS signals, and boxplots for 11 metabolites were drawn. LC–MS, liquid chromatography–mass spectrometry; LPC, lysophosphatidylcholine

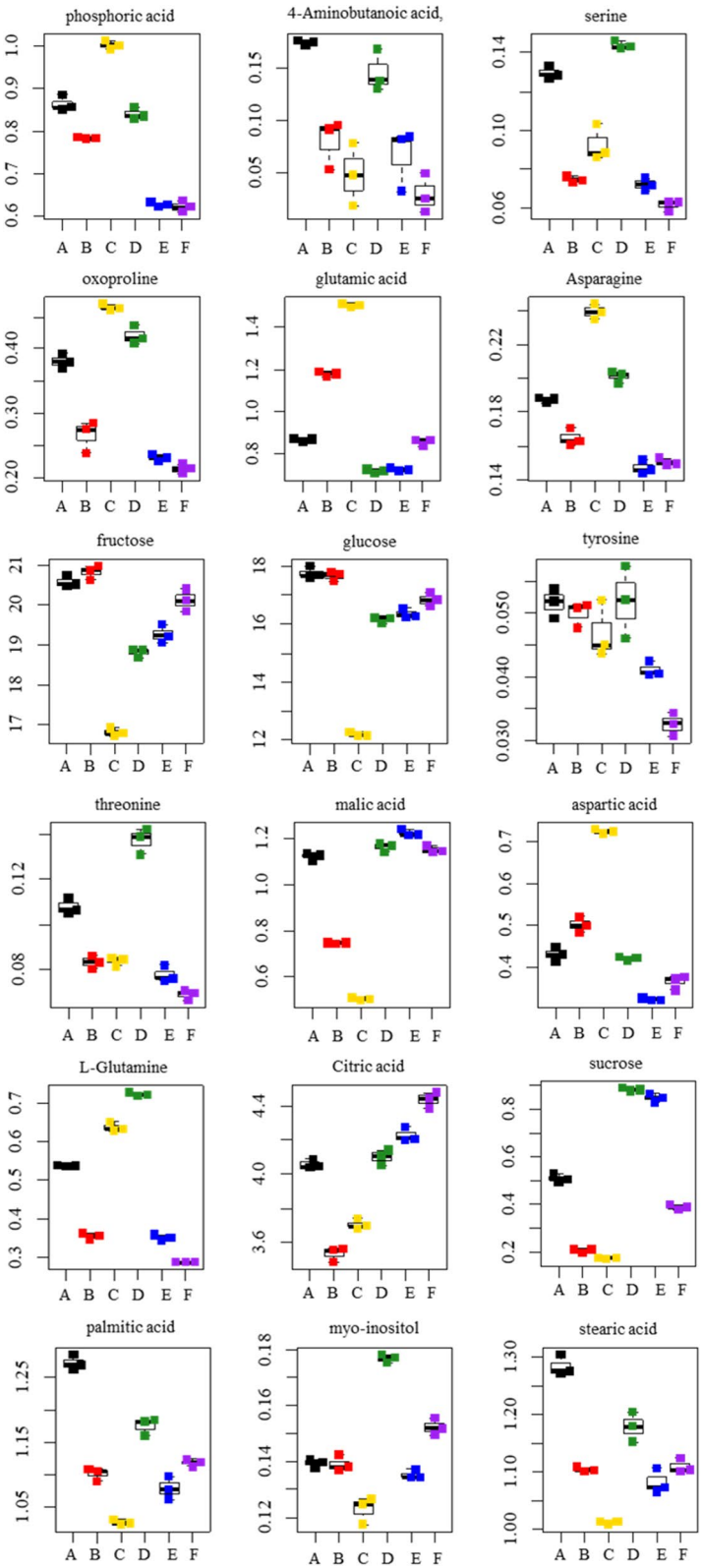

Fig. 5 Boxplot of each identified metabolite from GC–MS analyses. The 18 metabolites were quantified based on GC–MS signals, and boxplots for 18 metabolites were drawn. GC–MS, gas chromatography–mass spectrometry; LPC, lysophosphatidylcholine

Abbreviations

ACC	1-Aminocyclopropane-1-carboxylic acid
ACO	ACC oxidase
ACS	ACC synthase
BSTFA	N,O-bis (trimethylsilyl)trifluoroacetamide
CNR	Colorless non-ripening
GC–MS	Gas chromatography–mass spectrometry
LC–MS	Liquid chromatography–mass spectrometry
PLS-DA	Partial least squares-discriminant analysis
NOR	Non-ripening transcription factor
RI	Retention indices
RIN	Ripening inhibitors
VIP	Variable importance projection

Supplementary Information

The online version contains supplementary material available at https://doi.org/10.1186/s40543-023-00384-3.

Additional file 1: Fig. S1. The LC-MS chromatograms are shown from non-treated tomato samples with (**A**) 7 days ripening, (**B**) 10 days ripening, and (**C**) 14 days ripening. The LC-MS chromatograms from sound-wave treatment are shown in (**D**) 7 days ripening, (**E**) 10 days ripening, and (**F**) 14 days ripening.

Additional file 2: Fig. S2. The GC-MS chromatograms are shown from non-treated tomato samples with (**A**) 7 days ripening, (**B**) 10 days ripening, and (**C**) 14 days ripening. The GC-MS chromatograms from sound-wave treatment are shown in (**D**) 7 days ripening, (**E**) 10 days ripening, and (**F**) 14 days ripening.

Acknowledgements
Not applicable.

Author contributions
MJJ and BJK designed and conducted experiments and wrote the manuscript; JYK, MJJ, and BJK contributed to interpretation of data and conducted the experiments. All authors read and approved the final manuscript.

Funding
This study was supported by the NAS Agenda Program (Nos. PJ01501201 and PJ01501202) of the Rural Development Administration of Jeonju, Republic of Korea. This research was supported by Basic Science Research Program through the National Research Foundation of Korea (NRF) funded by the Ministry of Education (2021R1F1A106103413).

Availability of data and materials
Not applicable.

Declarations

Competing interests
The authors declare that they have no competing interests.

Received: 22 August 2022 Accepted: 6 April 2023
Published online: 04 July 2023

References

Abeles F, Page M, Saltveit M Jr. Ethylene in Plant Biology. Academic Press; 1992.
Agius C, von Tucher S, Poppenberger B, Rozhon W. Quantification of sugars and organic acids in tomato fruits. MethodsX. 2018;5:537–50.
Ara T, Sakurai N, Takahashi S, Waki N, Suganuma H, Aizawa K, et al. TOMATOMET: a metabolome database consists of 7118 accurate mass values detected in mature fruits of 25 tomato cultivars. Plant Direct. 2021;5(4):e00318.
Bochu W, Jiping S, Biao L, Jie L, Chuanren D. Soundwave stimulation triggers the content change of the endogenous hormone of the *Chrysanthemum* mature callus. Colloids Surf B Biointerfaces. 2004;37(3–4):107–12.
Choi B, Ghosh R, Gururani MA, Shanmugam G, Jeon J, Kim J, et al. Positive regulatory role of sound vibration treatment in *Arabidopsis thaliana* against *Botrytis cinerea* infection. Sci Rep. 2017;7(1):2527.
Fiedor J, Burda K. Potential role of carotenoids as antioxidants in human health and disease. Nutrients. 2014;6(2):466–88.
Gagliano M, Mancuso S, Robert D. Towards understanding plant bioacoustics. Trends Plant Sci. 2012;17(6):323–5.
Giovannoni JJ. Genetic regulation of fruit development and ripening. Plant Cell. 2004;16(Suppl):S170–80.
Guevara L, Domínguez-Anaya MÁ, Ortigosa A, González-Gordo S, Díaz C, Vicente F, et al. Identification of compounds with potential therapeutic uses from sweet pepper (*Capsicum annuum* L.) fruits and their modulation by nitric oxide (NO). Int J Mol Sci. 2021;22(9):4476.
Hoogstrate SW, van Bussel LJ, Cristescu SM, Cator E, Mariani C, Vriezen WH, et al. Tomato ACS4 is necessary for timely start of and progression through the climacteric phase of fruit ripening. Front Plant Sci. 2014;5:466.
Johnson PRE, Ecker JR. The ethylene gas signal transduction pathway: a molecular perspective. Annu Rev Genet. 1998;32:227–54.
Johnson KA, Sistrunk ML, Polisensky DH, Braam J. *Arabidopsis thaliana* responses to mechanical stimulation do not require ETR1 or EIN2. Plant Physiol. 1998;116(2):643–9.
Kesanakurti D, Kolattukudy PE, Kirti PB. Fruit-specific overexpression of wound-induced tap1 under E8 promoter in tomato confers resistance to fungal pathogens at ripening stage. Physiol Plant. 2012;146(2):136–48.
Kim JY, Lee J, Kwon T, Lee S, Kim JA, Lee G, et al. Sound waves delay tomato fruit ripening by negatively regulating ethylene biosynthesis and signaling genes. Postharvest Biol Technol. 2015;110:43–50.
Kim JY, Lee SI, Kim JA, Park S, Jeong M. Sound waves increases the ascorbic acid content of alfalfa sprouts by affecting the expression of ascorbic acid biosynthesis-related genes. Plant Biotechnol Rep. 2017;11(5):355–64.
Kim JY, Kang YE, Lee SI, Kim JA, Muthusamy M, Jeong MJ. Sound waves affect the total flavonoid contents in *Medicago sativa*, *Brassica oleracea* and *Raphanus sativus* sprouts. J Sci Food Agric. 2020;100(1):431–40.
Kim JY, Lee HJ, Kim JA, Jeong MJ. Sound waves promote *Arabidopsis thaliana* root growth by regulating root phytohormone content. Int J Mol Sci. 2021;22(11):5739.
Manning K, Tör M, Poole M, Hong Y, Thompson AJ, King GJ, et al. A naturally occurring epigenetic mutation in a gene encoding an SBP-box transcription factor inhibits tomato fruit ripening. Nat Genet. 2006;38(8):948–52.
Matto AK, Suttle JC. The plant hormone ethylene. 1st ed. Boca Raton: CRC Press; 1991.
Mun HI, Kwon MC, Lee NR, Son SY, Song DH, Lee CH. Comparing metabolites and functional properties of various tomatoes using mass spectrometry-based metabolomics approach. Front Nutr. 2021;8:659646.
Pan IL, McQuinn R, Giovannoni JJ, Irish VF. Functional diversification of AGAMOUS lineage genes in regulating tomato flower and fruit development. J Exp Bot. 2010;61(6):1795–806.
Shipman JT, Wilson JD, Higgins CA Jr, Lou B. An introduction to physical science. 14th ed. Cengage Learning, Inc.; 2016.
Takahashi H, Suge H, Kato T. Growth promotion by vibration at 50 Hz in rice and cucumber seedlings. Plant Cell Physiol. 1991;32(5):729–32.
Vrebalov J, Ruezinsky D, Padmanabhan V, White R, Medrano D, Drake R, et al. A MADS-box gene necessary for fruit ripening at the tomato ripening-inhibitor (rin) Locus. Science. 2002;296(5566):343–6.
Wang W, Vinocur B, Altman A. Plant responses to drought, salinity and extreme temperature: towards genetic engineering for the stress tolerance. Planta. 2003;218(1):1–14.
Wang R, Angenent GC, Seymour G, de Maagd RA. Revisiting the role of master regulators in tomato ripening. Trends Plant Sci. 2020;25(3):291–301.

Wishart DS. Metabolomics for investigating physiological and pathophysiological processes. Physiol Rev. 2019;99(4):1819–75.
Yang SFH, Hoffman NE. Ethylene biosynthesis and its regulation in higher plants. Annu Rev Plant Physiol. 1984;35(1):155–89.
Zhang WF, Gong ZH, Wu MB, Chan H, Yuan YJ, Tang N, et al. Integrative comparative analyses of metabolite and transcript profiles uncovers complex regulatory network in tomato (*Solanum lycopersicum* L.) fruit undergoing chilling injury. Sci Rep. 2019;9(1):4470.

Publisher's Note